Heliyon 8 (2022) e10938

Contents lists available at ScienceDirect

Heliyon

journal homepage: www.cell.com/heliyon

Research article

Potential impacts in soil slope of deformation and water content on elastic wave amplitude

Ming Xie [a], Jiahao Liu [a,*], Song Lu [b]

[a] School of Civil Engineering, Xi Jing University, Xi'an 710123, Shaanxi, China
[b] Quanzhou Institute of Equipment Manufacturing, Haixi Research Institute, Chinese Academy of Sciences, Quanzhou 362000, Fujian, China

ARTICLE INFO

Keywords:
Elastic wave
Landslides
Early warning
Rainfall-induced
Amplitude
EMD

ABSTRACT

Early warning during rainfall-induced landslides employs widely to save economic losses and casualties. Using elastic wave velocity for early warning benefits from the relationship between water content, shear deformation, and elastic wave velocity of unsaturated soil slope. Amplitude changes by means of the elastic wave in the soil can also reflect the physical properties. In this work, we proposed an idea to determine the impacts in the soil of water content and deformation on elastic wave amplitude to realize early warning. Model box tests were designed to study the action of one factor, volumetric water content, on the elastic wave amplitude. Slope model tests were aimed to consider the effects of volumetric water content and deformation on elastic wave amplitude during rainfall-induced landslides. The results show that the elastic wave amplitude non-linear decreased with the volumetric water content, which could be mutually verified from the data of the model box tests and the slope model tests. The deformation caused the wave amplitude to increase, and the range of the increase could reflect the range of the deformation. The statistical correlation coefficient quantified that the increase in wave amplitude was not directly related to the water content. The wave amplitude change can be represented more visibly by eliminating the residual after EMD decomposition, and it further verifies the above results. This work provides a new idea and a reliable basis for landslide prevention and mitigation and prediction.

1. Introduction

Various causes impact landslides, the most significant of which is rainfall, and they pose a serious threat to people's lives and property all over the world (Montoya-Domínguez et al., 2016; Notti et al., 2021; Ochiai et al., 2004; Wu et al., 2015; Xiao et al., 2020). Rainfall induced about 63% of the landslides between 1999 and 2012, according to data from 134 landslides (www.glidenumber.net). The demand for preventing and controlling rainfall-induced slope instability is growing daily. However, traditional landslide control approaches are not always feasible because of cost and construction, especially when huge regions need to be covered (Chen and Uchimura, 2019a; Uchimura et al., 2010). Monitoring and early warning of rainfall-induced landslides cannot wholly prevent a landslide. Still, it can substantially reduce the risk and assure life safety and has been widely adopted as a cost-effective and reliable option (Lollino et al., 2002; Wu et al., 2019; Xu et al., 2016). Li et al. improved a region growing segmentation method for the image recognition of the deformation area of open-pit mine rock slopes, which may be applied to identify rock slope deformation in complex scenes with high precision and enhances the reliability of early warning (Li et al., 2022). Guo et al. proposed a black box model based on statistical analysis, which may provide a basis for early warning of creep landslides through practical application results in China (Guo et al., 2019). A physics-based model by Medina et al. was developed, called the "Fast Shallow Landslide Assessment Model" (FSLAM), for calculating large areas (>100 km (2)) with a high-resolution topography in a very short computational time, thereby greatly improving the warning results (Medina et al., 2021).

Most landslide warning systems give alerts by defining thresholds for physical soil properties like rainfall, volumetric water content, slope movement, etc. The drawback of using rainfall thresholds is determined based on the magnitude of rainfall from previous landslide events rather than the physical properties of soil (Baum and Godt, 2010). The volumetric water content and slope movement thresholds depend on sensors, which are only sensitive to changes on their own around and cannot cover the entire soil slope (Chae and Kim, 2012; Uchimura et al., 2015). Acoustic emission is limited by its signal of weak and rapidly debilitating, which affects the efficiency of early warning (Dixon et al., 2015a,b;

* Corresponding author.
E-mail address: iu20210428@hotmail.com (J. Liu).

https://doi.org/10.1016/j.heliyon.2022.e10938
Received 26 April 2022; Received in revised form 8 June 2022; Accepted 29 September 2022

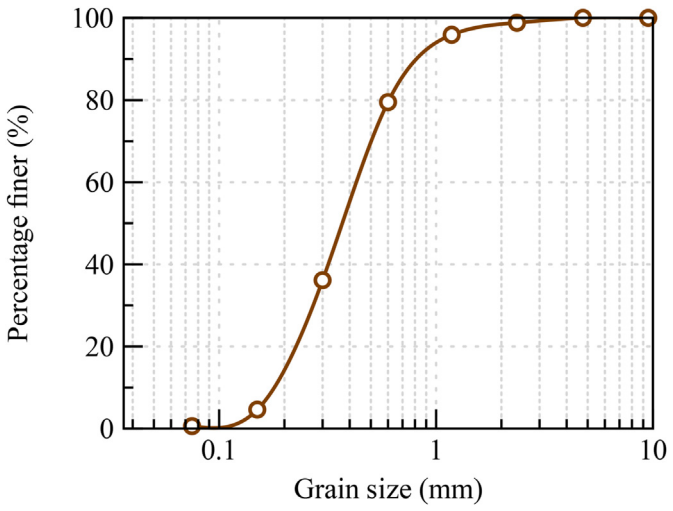

Figure 1. Particle size distribution of test material.

Table 1. Physical properties of test material.

Properties	Test material
Specific gravity, G_s	2.575
Mean grain size, D_{50} (mm)	0.373
Coefficient of uniformity, C_u	2.641
Coefficient of gradation, C_c	0.946
Fines content (%)	16.1
Maximum void ratio, e_{max}	1.47
Minimum void ratio, e_{min}	0.98
Maximum dry density (g/cm^3)	1.717
Optimum moisture content (%)	16.1

Dixon and Spriggs, 2007; Minakov and Yarushina, 2021). At present, it's challenging work to accurately achieve early warning during rainfall-induced landslides on a broad scale.

The elastic wave is discovered to carry a lot of information about the physical properties in the soil, which can directly represent the influence of changing boundary conditions on slope behavior (Chen and Uchimura, 2019b). Irfan et al. investigated the relationship between elastic wave velocity with soil moisture content and deformation in laboratory triaxial tests employing the bender element, in which the elastic wave velocity decreases with volumetric water content, and it accelerated decreases at slope failure (Irfan, 2014; Irfan et al., 2017; Irfan and Uchimura, 2013,

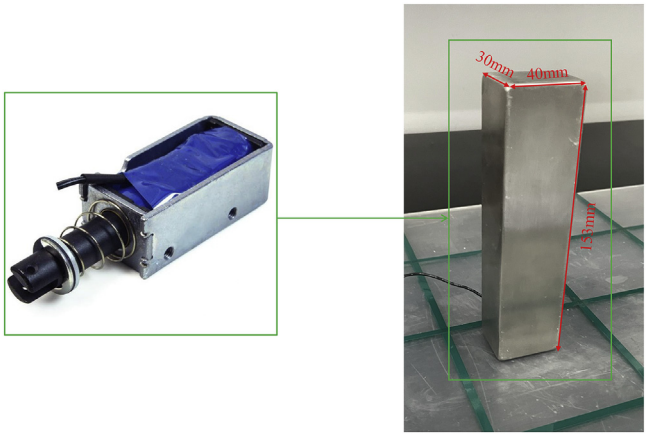

Figure 2. Elastic wave exciter.

Table 2. Characteristics of model box tests.

Test designation	Dry density (g/cm^3)	Water content (%)	Duration (min)
1-1.2-5	1.2 (D_c = 69.4%)	5	10
1-1.2-10		10	
1-1.2-20		20	
1-1.3-5	1.3 (D_c = 72.1%)	5	
1-1.3-10		10	
1-1.3-20		20	
1-1.4-5	1.4 (D_c = 79.4%)	5	
1-1.4-10		10	
1-1.4-20		20	

2015, 2016, 2018). According to this point, Chen Yulong et al. studied the change of elastic wave velocity during rainfall-induced slope instability by slope model tests and verified its practical usefulness (Chen, 2016; Chen et al., 2017, 2018a, 2018b, 2019). Due to the rapid propagation of elastic waves in the soil, a high sample frequency is required for the data acquisition unit, resulting in a high cost of the elastic wave monitoring system. At the same time, the development of the elastic wave velocity calculation, and observation method, is still inadequate.

In this work, an idea to use elastic wave amplitude for early warning during rainfall-induced landslides was presented. Amplitude information

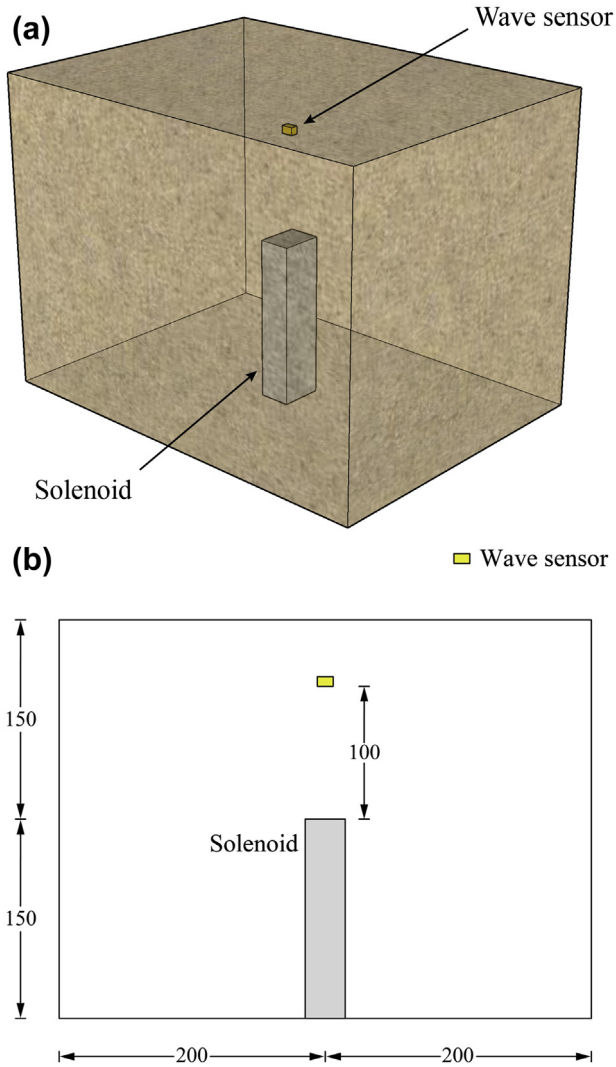

Figure 3. The schematic of model box: (a) 3D illustration, (b) scaled 2D model.

is an indicator of the elastic wave energy, which change is influenced by the physical properties of the soil (Cheng and Yang, 2005; Guo et al., 2007; Han and Zhang, 2006; Yang et al., 1996; Zhang, 2018). The volumetric water content and slope movement/deformation in the soil constantly change during rainfall infiltration, leading to different consumption of elastic wave energy. The sampling frequency of the data acquisition unit required to calculate the elastic wave amplitude is low, and the wave amplitude calculation is simple. Model box tests were first conducted to study the effect of one factor, volumetric water content, on the elastic wave amplitude, without considering deformation. Slope model tests were employed to study the amplitude changes during rainfall-induced landslides, taking into account water content and deformation. Also, soils with different dry densities were done in both tests to show that the water content and deformation consistently contribute to the elastic wave amplitude at any density. Finally, the influence of volumetric water content and deformation on amplitude was analyzed in detail by combining empirical mode decomposition (EMD). The research results will provide an essential reference for the landslide warnings based on elastic wave amplitude.

2. Method of model tests

2.1. Material and instruments

One sand, from a coastal area in Fujian, was used as testing material: the sand particles with smooth surface, rounded grain shape, and large permeability coefficient. Figure 1 and Table 1 show particle size distribution and basic soil properties of the test material measured according to the geotechnical test method standards (GB/T50123-2019), respectively.

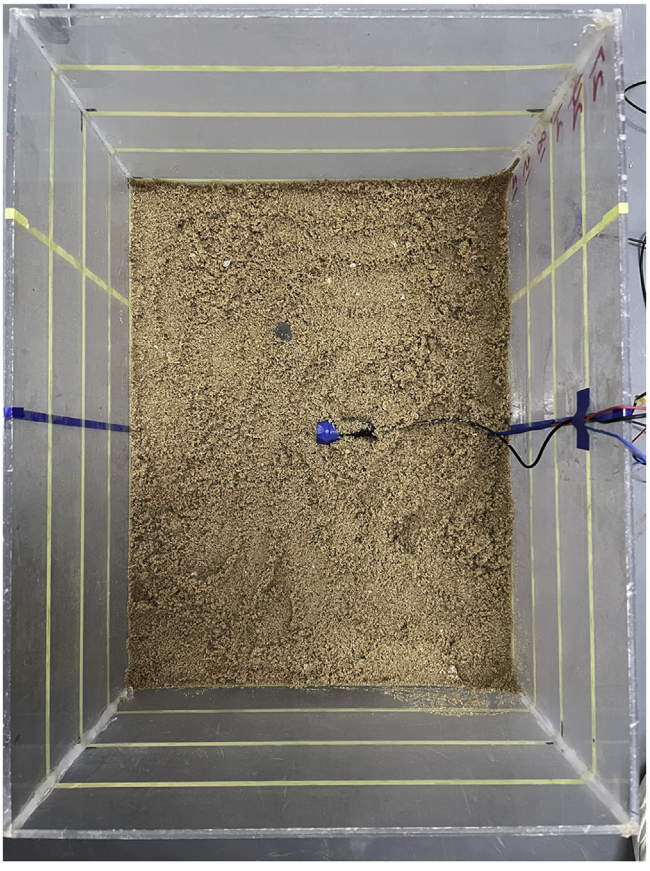

Figure 4. Layered accumulation and compaction of the model during the model box tests.

Table 3. Characteristics of slope model tests.

Test designation	Slope angle (°)	Surface layer thickness (mm)	Rainfall duration (min)	Dry density (g/cm^3)
2-45-10-1.2	45	10	60	1.2 (D_c = 69.4%)
2-45-10-1.3				1.3 (D_c = 72.1%)
2-45-10.1.4				1.4 (D_c = 79.4%)

Several types of instrumentation in tests were included with an elastic wave monitoring system, soil moisture sensors, and rainfall simulator. The elastic wave monitoring system consisted of an exciter, receivers, a microcontroller, and a data acquisition unit. A solenoid was applied as an elastic wave exciter, which has an internal iron core that makes a stable elastic wave signal by current action and was protected by metal on all sides so that stable work can be achieved in soil. Figure 2 shows that the left side is the original solenoid, and the other side is the elastic wave exciter (the solenoid protected by metal all around). The microcontroller adjusted the work hours of the exciter to one group per minute, and it worked 5 times at intervals of 10 s in each group. A data acquisition unit and receivers were used to record and measure elastic wave signals, that were denoised by a combination of superposition denoising and wavelet threshold denoising. Soil moisture sensors, connecting to a data acquisition unit, were used to monitor volumetric water content in tests. Rainfall simulators as artificial rainfall equipment could produce a uniform distribution.

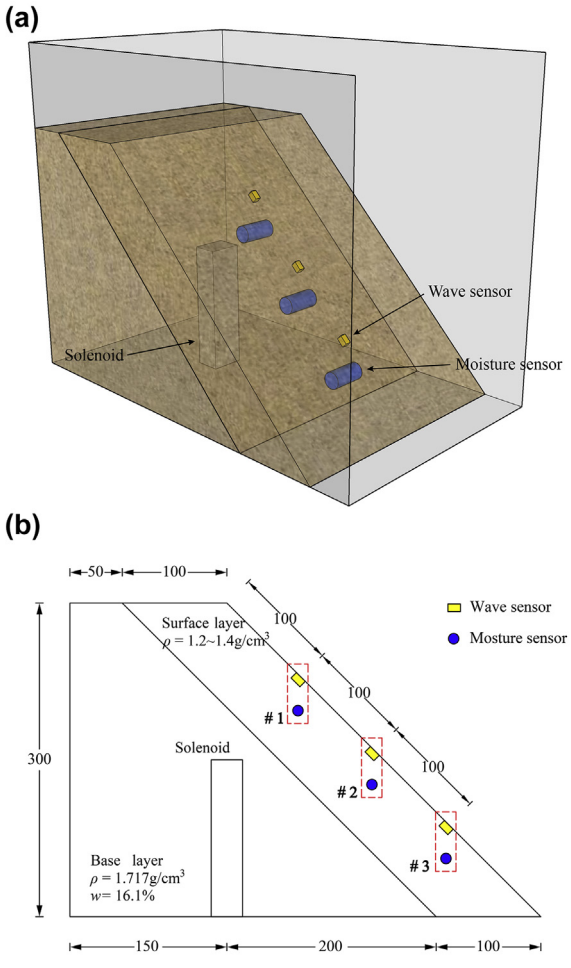

Figure 5. The schematic of slope model: (a) 3D illustration, (b) scaled 2D model.

2.2. Testing scheme

2.2.1. Model box tests

The model box tests reveal the action of volumetric water content on the elastic wave amplitude by manually controlling the soil with water content without considering other factors such as deformation. Also, the control group of soils with different densities aims to indicate a consistent effect of volumetric water content on the elastic wave amplitude at any density. Nine tests were designed for the model box tests. Table 2 shows the summary of the test schemes. The first column of Table 2 systematically indicates test designation, dry density (in g/cm^3), water content (in %), and duration (in minutes). The dry densities of the soil samples in the box tests are 1.2, 1.3, and 1.4 g/cm^3 (D_c = 69.4%, 72.1%, and 79.4%, respectively), moisture contents of the soil samples in the box tests are 5%, 10%, and 20%.

The model in model box tests was 400 mm in length, 300 mm wide, and 300 mm high, and the container was made of plexiglass 5 mm thick, as shown in Figure 3. The exciter was located at the bottom of the model, and which plunger movement direction was perpendicular to the level. The receiver was put 100 mm above the exciter. The model was made by layered accumulation and compaction, as shown in Figure 4. The working interval of the exciter was 10-s, and the sampling frequency of the elastic wave signal was adjusted to 5 kHz. The duration of the model box tests was 10 min, during which the elastic wave signals were recorded continuously.

2.2.2. Slope model tests

The slope model tests simulate rainfall-induced landslides to study the relationship between water content and peristaltic deformation with elastic wave amplitude in the soil during landslides. Three tests were designed for the slope model tests. Table 3 shows the summary of the test schemes. The first column of Table 3 systematically indicates test designation, slope inclination angle (in degrees), surface layer thickness (in millimeters), rainfall duration (in minutes), and dry density (in g/cm^3).

The model in slope model tests was 450 mm in length, 300 mm wide, and 300 mm high, which was divided into a base layer and surface layer, and the container was made of plexiglass 5 mm thick, as shown in Figure 5. Slope model angles of 40° were used. The maximum dry density of 1.717 g/cm^3 (D_c = 97.2%) and optimum moisture content of 16.1% were adopted at the base layer. The thicknesses of surface soil layers were 100 mm, and dry densities of the soil samples were 1.2, 1.3, and 1.4 g/cm^3 (D_c = 69.4%, 72.1%, and 79.4%, respectively).

The exciter was fixed to the bottom of the base soil layer. Plunger movement direction was perpendicular to level. The receivers and moisture sensors amount to three, respectively, and were placed on the surface soil layer, and the receivers were limited to the measurement range of the moisture sensors. The soil moisture variations and elastic wave signal were measured at 1-s intervals and 10-s intervals during the entire test, respectively. The rainfall was 100 mm/h for 60 min, during which the water content and elastic wave were recorded continuously. The receivers were numbered EWA, and the volumetric water content sensors were numbered VWC during the tests.

3. Results and discussion

3.1. Model box tests

Figure 6 depicts the change of elastic wave amplitude in different dry densities with volumetric water content. In all three different dry density tested cases, the elastic wave amplitude decreased with volumetric water content.

The amplitude decreased nonlinearly with volumetric water content, and this trend was observed in soil samples with each dry density. This increase in volumetric water content meant that the pores inside the soil were filled with water, which increased the loss of elastic wave energy and thus decreased the elastic wave amplitude. The elastic wave amplitude increased with dry density during the same volumetric water content. This increase was because of the compactness between soil particles, which greatly increased the energy transfer of the elastic wave.

It could be inferred that volumetric water content was a crucial factor in changing elastic wave amplitude. And it did not induce a mutation in amplitude but a non-linear decline. The greater the water content, the less pronounced the decrease in elastic wave amplitude. Based on the relationship between volumetric water content and elastic wave amplitude, the slope model tests would consider additional slope movement, that deformation.

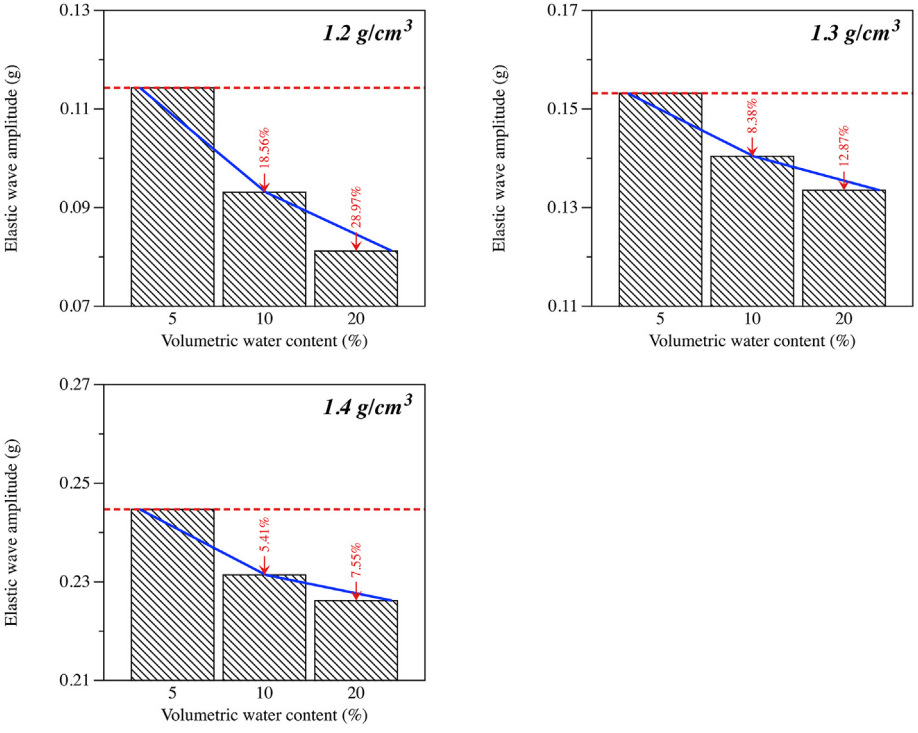

Figure 6. Change of elastic wave amplitude in different dry densities with volumetric water content by model box tests.

3.2. Slope model tests

During rainfall-induced landslides, the volumetric water content and deformation increased in slopes and were accompanied by sudden cracking. Figure 7 describes the time series of elastic wave amplitude and water content in slope model tests. Figure 8 represents the slope failure process for test cases 2-45-10-1.3. Due to the moisture was penetrated in surface with rainfall and the water content gradually increased. At the same time, creeping deformation was accompanied inside the slope. The water content was raised differently at different locations on the slope,

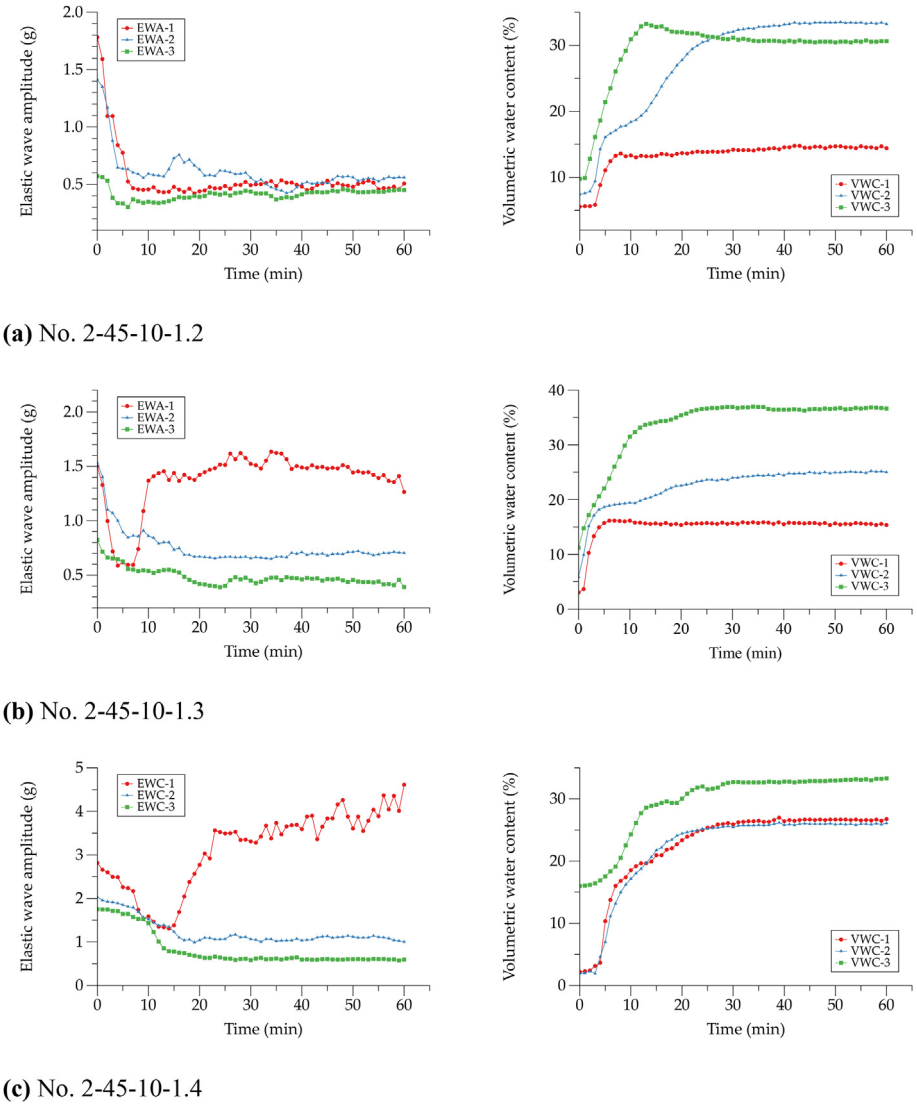

Figure 7. Change in time series data of elastic wave amplitude and volumetric water content by slope model tests: (a) No. 2-45-10-1.2, (b) No. 2-45-10-1.3, (c) No. 2-45-10-1.4.

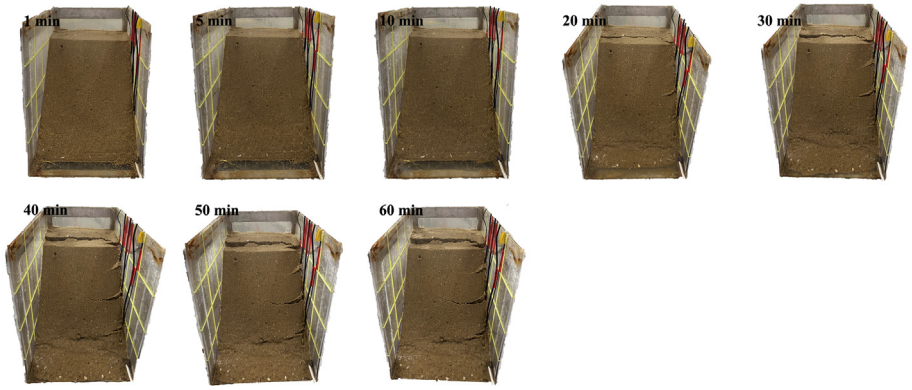

Figure 8. Slope failure process during test No. 2-45-10-1.3.

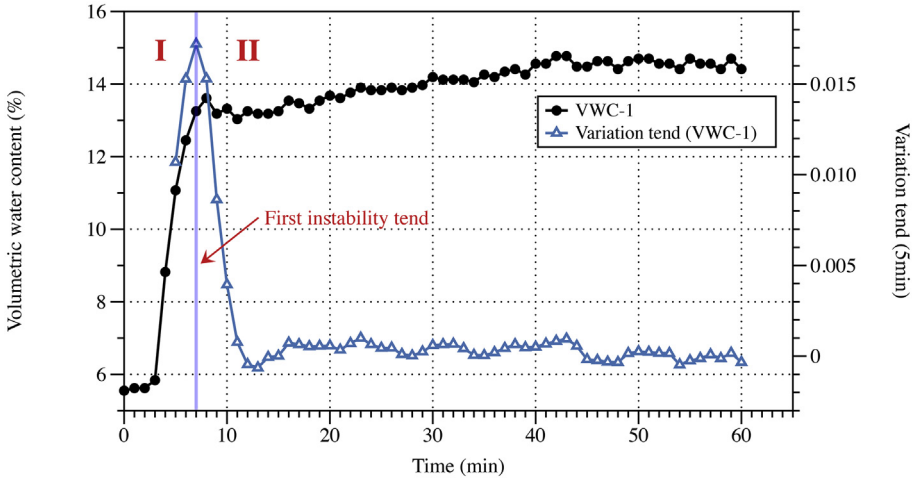

Figure 9. Slope first instability tend during test No. 2-45-10-1.2 # 1.

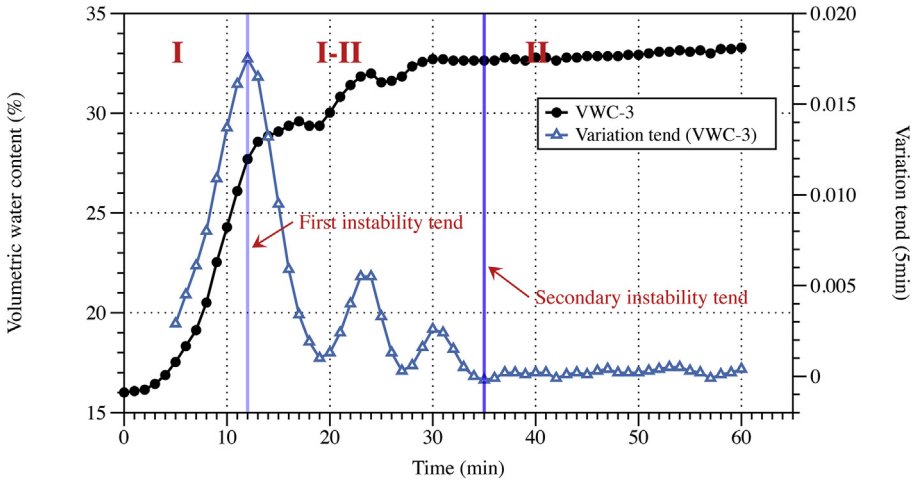

Figure 10. Slope first and secondary instability tend during test No. 2-45-10-1.3 # 3.

and the maximum water content varied, which was reflected in the slope model tests of different dry densities. These were influenced by factors such as infiltration and runoff. The water contents in the lower part of the slopes (#3) were the first to increase, forming a groundwater level. The rise of the groundwater level led to an increase in the water contents in the middle parts (#2) and upper parts (#1) of the slopes.

3.2.1. Temporal quantification of the soil slopes instability trend

The volumetric water content in the soil slopes raised during rainfall infiltration, the pore water pressure increased, and the effective stress in the unsaturated zone decreased. These led to changes in the internal structure of the slopes and increased landslide risk. The volumetric water content could reflect the physical information inside the soil slope, and it

Table 4. Time domain division of slope stability trend.

Test designation		I stage (min)	First instability tend (min)	I–II stage (min)	Secondary instability tend (min)	II stage (min)
2-45-10-1.2	#1	0–6	7	–	–	7–60
	#2	0–5	6	6–39	40	40–60
	#3	0–5	6	–	–	6–60
2-45-10-1.3	#1	0–4	5	–	–	5–60
	#2	0–4	5	5–28	29	29–60
	#3	0–4	5	–	–	5–60
2-45-10-1.4	#1	0–7	8	–	–	8–60
	#2	0–7	8	8–33	34	34–60
	#3	0–11	12	12–36	37	37–60

Table 5. Statistical information in relevance in the **I** stage.

Test designation		Person correlation	Spearman correlation	R^2
2-45-10-1.2	#1	−0.8324	−0.9910	0.7093
	#2	−0.9165	−1	0.8856
	#3	−0.9639	−1	0.9401
2-45-10-1.3	#1	−0.9897	−1	0.9518
	#2	−0.9930	−1	0.9556
	#3	−0.9506	−1	0.9485
2-45-10-1.4	#1	−0.9105	−1	0.9043
	#2	−0.8753	−0.8982	0.8102
	#3	−0.9727	−1	0.9365

Correlation was significant at -0.6 level.

was defined as the index to analyze the stability of the soil slopes under time series. When the volumetric water content growth decreased significantly, it meant that the soil slope was ruptured and fissures existed; when the volumetric water content oscillated slightly and tended to be smooth, it meant that the soil slope was saturated with water content. Both of the above result in increased landslide risk.

The trend of the volumetric water content under the time series was calculated with a time unit width of 5 min. The soil slopes were considered saturated when the variation trend of volumetric water content reached its highest point, which was defined as the first instability trend. Before this, the main factor affecting the elastic wave amplitude was the volumetric water content, which was determined as the **I** stage. After which there were two situations: the trend of the volumetric water content gradually decreased and became stable, and the main factor affecting the elastic wave amplitude was deformation, which was defined as the **II** stage; the trend of the volumetric water content decreased and

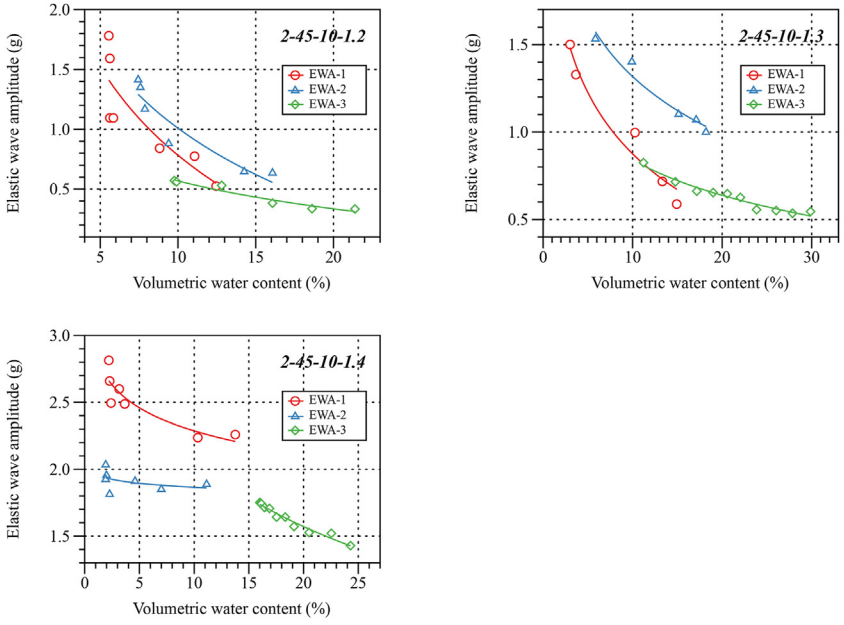

Figure 11. Relationship between the volumetric water content and the elastic wave amplitude during the **I** stage.

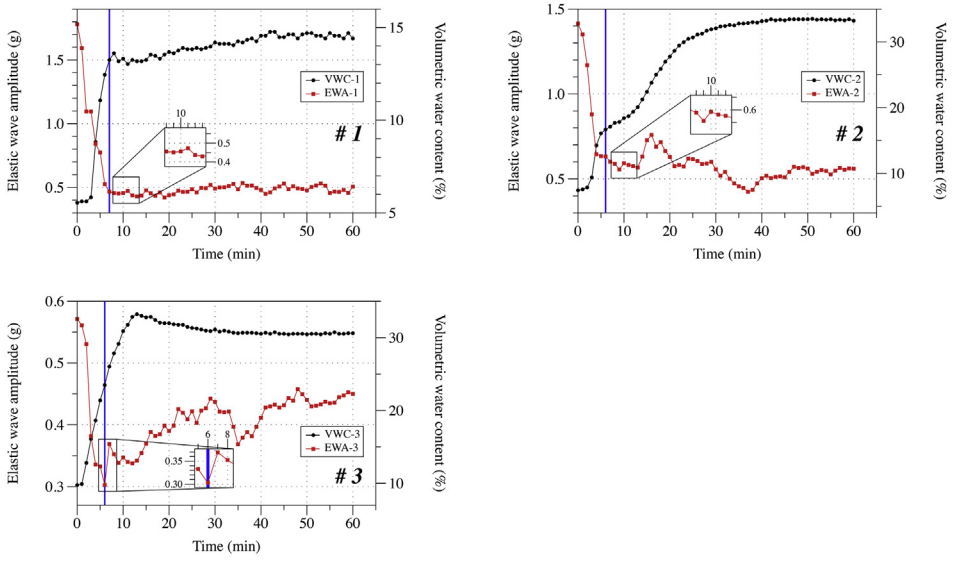

Figure 12. Change in time series data of elastic wave amplitude and volumetric water content during test No. 2-45-10-1.2.

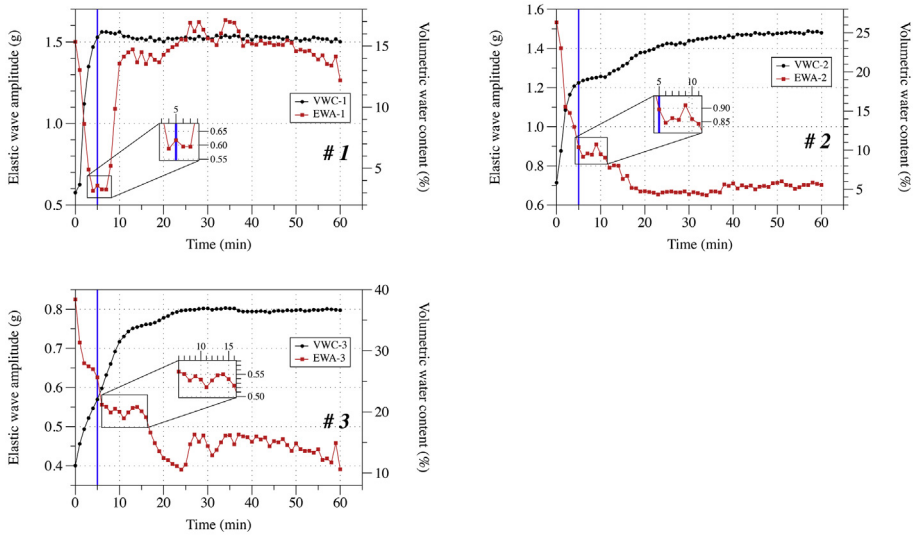

Figure 13. Change in time series data of elastic wave amplitude and volumetric water content during test No. 2-45-10-1.3.

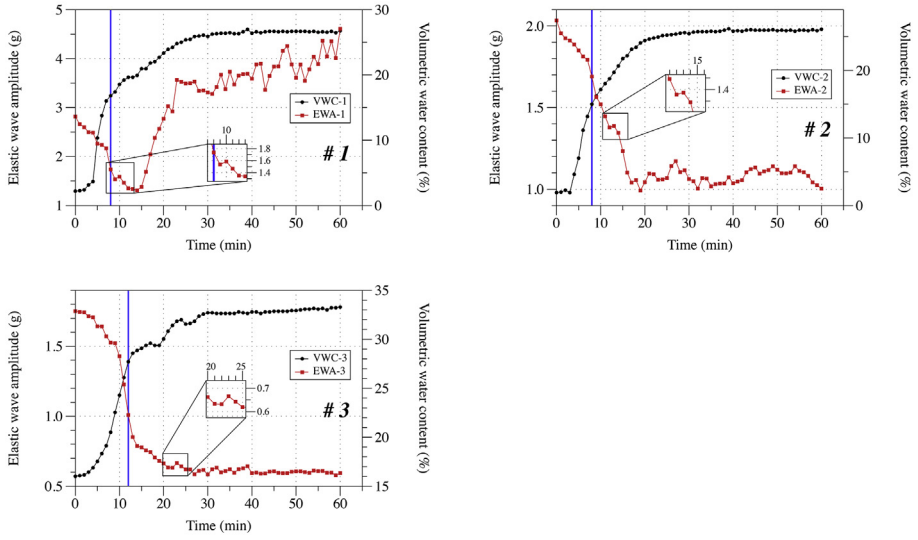

Figure 14. Change in time series data of elastic wave amplitude and volumetric water content during test No. 2-45-10-1.4.

then repeatedly increased and decreased, and the continuous deformation of the soil slope was not obvious, water content and deformation were mutually coupled to influence the elastic wave amplitude, which was defined as **I–II** stage. The **I–II** stage would gradually transition to the **II** stage, with a secondary instability trend at the point where the trend in volumetric water content plateaus (as shown in Figures 9 and 10, for example, 2-45-10-1.2 # 1 and 2-45-10-1.3 # 3, respectively). Table 4 shows the stage of slope development for each test.

Table 6. Statistical information in relevance in the **I–II** stage and **II** stage.

Test designation		I–II stage		II stage	
		Person correlation	Spearman correlation	Person correlation	Spearman correlation
2-45-10-1.2	#1	–	–	0.5258	0.4561
	#2	−0.4803	−0.6344	0.3696	0.3509
	#3	–	–	0.1465	−0.3702
2-45-10-1.3	#1	–	–	−0.437	0.1064
	#2	−0.9595	−0.9193	0.6918	0.5806
	#3	–	–	−0.7728	−0.4835
2-45-10-1.4	#1	–	–	0.937	0.8616
	#2	−0.941	−0.6015	0.23	0.2982
	#3	−0.8777	−0.8427	−0.348	−0.0803

Correlation was significant at −0.6 level.

3.2.2. I stage

Table 5 and Figure 11 show the correlation information and fitted curves between the water content and the wave amplitude in the **I** stage, respectively. Two correlation coefficients (Pearson product-moment correlation coefficient and Spearman rank correlation) and the fitted curves were used to measure the relationship between the water content and the wave amplitude from different points of view. All Pearson and Spearman coefficients reached high negative correlation levels, some even reaching-1. This was compared with the result of the model box tests, the elastic wave amplitude decreased with the volumetric water content, which was verified with each other. The fitted curves between the volumetric water content and the elastic wave amplitude described the non-linear characteristics of both. It was the same result as the model box tests. During the **I** stage, the elastic wave amplitude behaved as a non-linear decrease with the volumetric water content, and the soil slopes had certain stability, but their risk of damage is gradually increasing.

3.2.3. I–II stage and II stage

Figures 12, 13, and 14 show the time series results of the slope model tests, with the solid blue lines being the first instability trend and the secondary instability trend, respectively. The elastic wave amplitude was coupled with the volumetric water content and deformation during the **I–II** stage. During the **I–II** stage, the volumetric water content gradually increased as the rainfall continues. The general trend of the elastic wave amplitude was decreased, but there was an intermittent increase. During the **II** stage, the volumetric water content reached saturation, and the elastic wave amplitude appeared to rise disorderly. Since the volumetric water content could only cause a nonlinear decrease in wave amplitude, it was not difficult to speculate that the increase in wave amplitude was caused by deformation.

Table 6 shows the correlation information during the **I–II** stage and **II** stage between the water content and the wave amplitude. A few test cases in the **I–II** stage were represented that the correlation between volumetric water content and elastic wave amplitude was significant. But it was significantly lower than the result obtained in the **I** stage, which might be due to deformation. There was no obvious negative correlation between the volumetric water content and the elastic wave amplitude during the **II** stage, and the elastic wave amplitude increased on a large scale. At this time, the volumetric water content was nearly saturated, and the increase in the amplitude was not caused by the water content.

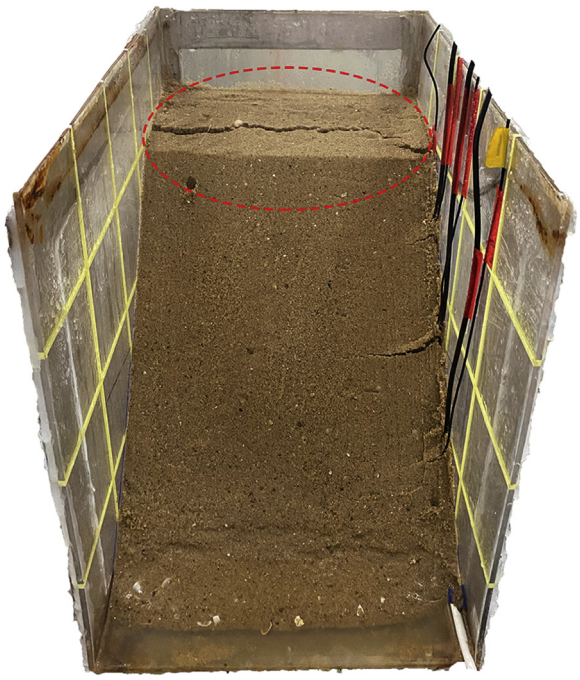

Figure 16. Slope failure in the **I–II** stage or **II** stage during No. 2-45-10-1.3.

Figure 15 illustrates that deformation affects the increase of the wave amplitude from the perspective of the relationship between the volumetric water content and the wave amplitude. During the **I–II** stage and **II** stage, the soil slope had the possibility of cracking at any time, and the soil slope developed from a homogeneous state to a non-homogeneous state continuously. In which the elastic wave

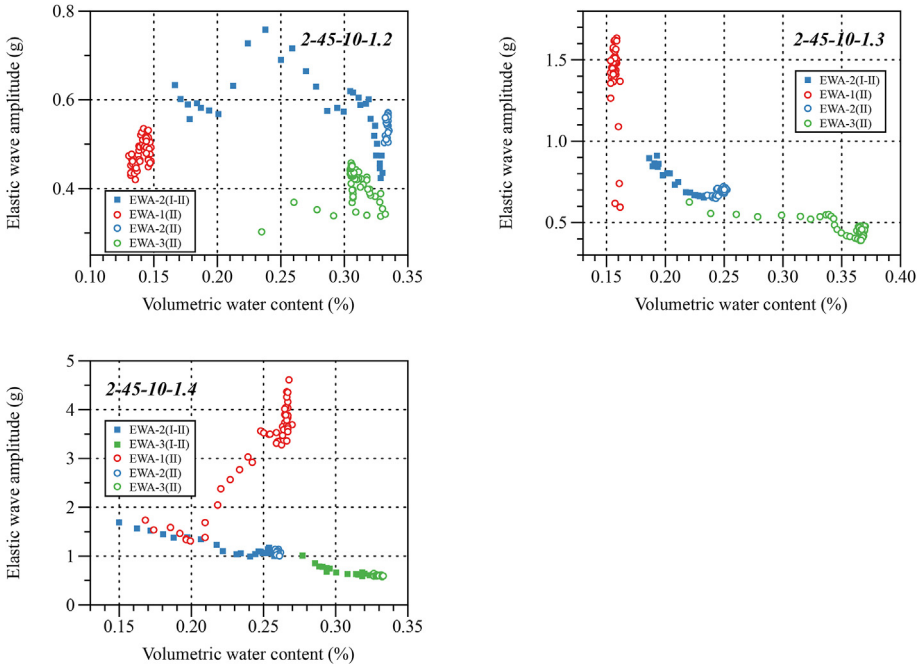

Figure 15. Relationship between the volumetric water content and the elastic wave amplitude during the **I–II** stage and **II** stage.

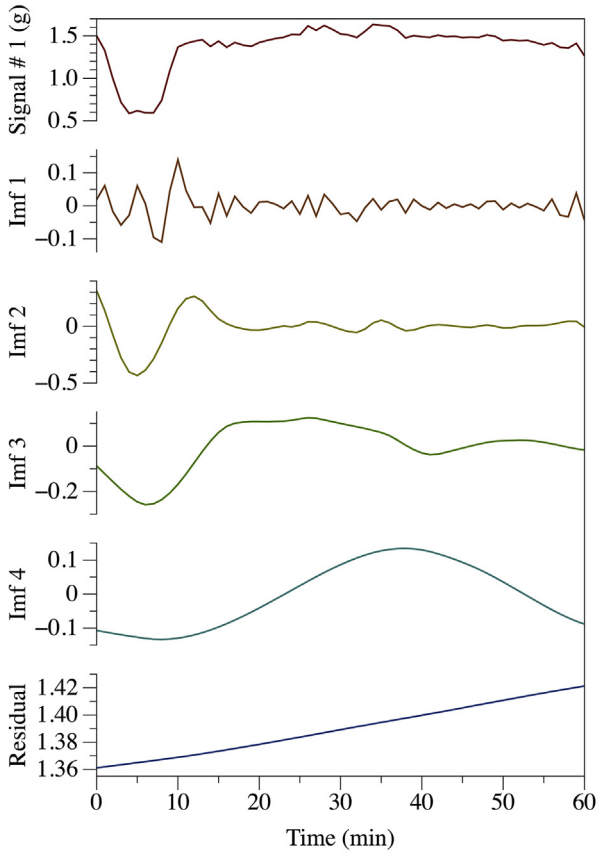

Figure 17. These IMFs and Residue for the wave amplitude data from # 1 in test No. 2-45-10-1.3 derived through EMD.

signal collected was interfered with by distortion. The deformation of the soil could be judged by the magnitude of the increase in wave amplitude. A small increase indicated creep within the soil slope, and an accelerated increase indicated a large crack in the soil slope. The large cracking of the soil slope could be observed in Figure 16, which corresponded to the time point of the accelerated increase of the elastic wave amplitude collected by EWA-1.

3.3. Discussions by empirical mode decomposition (EMD)

Empirical Modal decomposition (EMD), a signal decomposition method, has been suggested for processing the data (Huang et al., 2003a, b; Wang et al., 2018; Yang, 2015). It was proposed by Huang et al. to be a novel data analysis method for nonlinear and non-stationary time series (Huang et al., 1998). Zhang et al. analyzed crude oil price data by Ensemble EMD (EEMD), which is shown to be a vital technique (Zhang et al., 2008).

The wave amplitude data were discussed by EMD to further study elastic wave amplitude variation during rainfall-induced landslides. Take S-10-45-1.3 # 1 as an example, results of the EMD are depicted in Figure 17, which includes IMFs and a Residual. These IMFs showed detailed information about the variation of wave amplitude at different frequencies, and Residual represented the trend of wave amplitude variation during rainfall-induced landslides. The relative information of the wave amplitude variation was obtained by eliminating the residual after EMD decomposition.

Figure 18 shows the time domain information on the relative change of the elastic wave amplitude, with the solid blue lines being the first instability trend and the secondary instability trend, respectively. The amplitude data processed by EMD clearly highlights the change of amplitude and is more sensitive to the fluctuation of the data. During the **I** stage, the relative wave amplitude change was negative, and the soil slope did not show significant deformation. During the **I–II** stage and **II** stage, the increase of the relative wave amplitude change implied the deformation of the soil slope. The larger the value was, the more serious the soil slope deformation was. The large cracking was most visible at # 1, when the amplitude had an accelerated increase in the time domain. The first failure of the soil slope was in the **I–II** stage or **II** stage. And the data of relative change of wave amplitude could accurately locate its time point. If the relative change in elastic wave amplitude could be monitored in real-time, reliable information on water content change and slope deformation could be obtained, resulting in early warning.

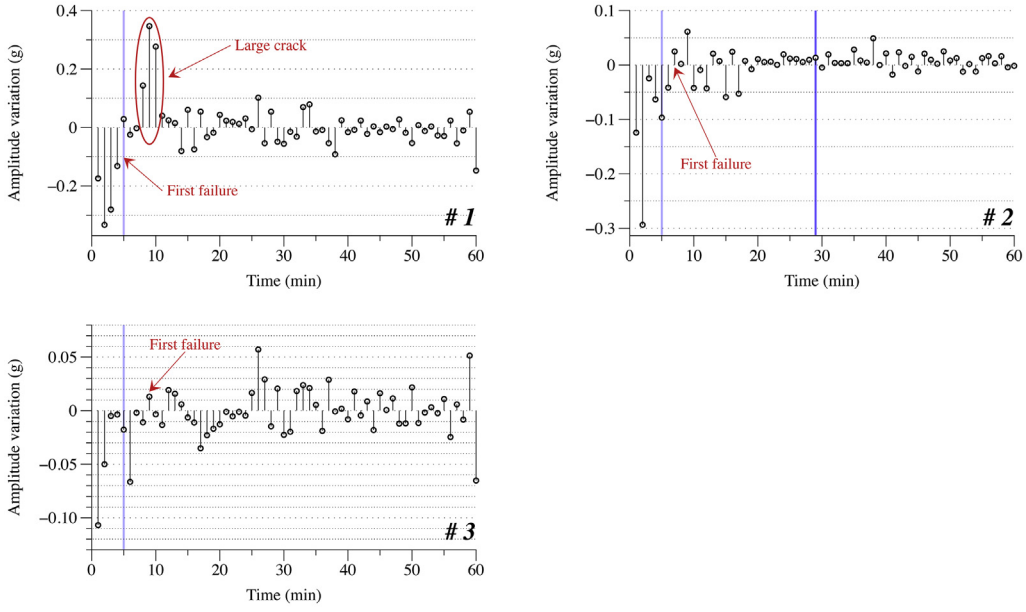

Figure 18. Relative change of elastic wave amplitude in test No. 2-45-10-1.3.

4. Conclusions

A landslide warning mechanism based on elastic wave amplitude was proposed in this work. The model box tests were used to study the effect of one factor, volumetric water content, on elastic wave amplitude. In different dry densities, the elastic wave amplitude all showed a non-linear decrease with the volumetric water content. There was no accelerated change in wave amplitude created by the change in volumetric water content. The slope model tests were intended to consider the impacts of the volumetric water content and deformation on the elastic wave amplitude during rainfall-induced landslides. During the **I** stage, the water content was the most critical component to decrease the elastic wave amplitude, which was mutually verified with the results of the model box tests. The statistical correlation coefficients and R^2 further quantitatively confirmed the non-linear decrease of the elastic wave amplitude with the volumetric water content. During the **I–II** stage and **II** stage, the volumetric water content and deformation combined to affect the elastic wave amplitude. The statistical correlation coefficient quantified that the increase in wave amplitude was not directly related to the water content. Also, the elastic wave amplitude was accelerated to increase when huge cracks were found in the slope. The increased range of the elastic wave amplitude could represent the extent of deformation in the slope. The elastic wave amplitude changes in the different dry densities surface layer during slope model tests all showed the above characteristics.

The wave amplitude data by EMD were analyzed to show the change of soil moisture content and deformation more prominently and detected creeping deformation and cracking during rainfall-induced landslides. During the **I–II** stage or **II** stage, the increase of the relative wave amplitude change implied the deformation of the soil slope, and the larger the value the more serious the deformation of the soil slope. It is recommended that the relative change of elastic wave variation be monitored in real-time to provide an early warning in the first moment of creeping deformation.

Declarations

Author contribution statement

Ming Xie: Conceived and designed the experiments; Contributed reagents, materials, analysis tools or data; Wrote the paper.

Jiahao Liu: Conceived and designed the experiments; Performed the experiments; Analyzed and interpreted the data; Wrote the paper.

Song Lu: Conceived and designed the experiments; Analyzed and interpreted the data; Contributed reagents, materials, analysis tools or data.

Funding statement

This research did not receive any specific grant from funding agencies in the public, commercial, or not-for-profit sectors.

Data availability statement

Data will be made available on request.

Declaration of interest's statement

The authors declare no conflict of interest.

Additional information

No additional information is available for this paper.

References

Baum, R.L., Godt, J.W., 2010. Early warning of rainfall-induced shallow landslides and debris flows in the USA. Landslides 7, 259–272.
Chae, B.-G., Kim, M.-I., 2012. Suggestion of a method for landslide early warning using the change in the volumetric water content gradient due to rainfall infiltration. Environ. Earth Sci. 66, 1973–1986.
Chen, Y., 2016. Changes in Elastic Wave Velocity in a Slope Due to Water Infiltration and Deformation (Ph.D.). The University of Tokyo, Tokyo, Japan.
Chen, Y., Uchimura, T., 2019a. Model tests of evaluation behaviors of the elastic wave velocity during the failure process of soil slopes due to rainfall. Chin. J. Rock Mech. Eng. 38, 2138–2150.
Chen, Y., Uchimura, T., 2019b. Early warning of rainfall-induced landslides based on elastic wave velocity. Rock Soil Mech. 40, 3373–3386.
Chen, Y., Uchimura, T., Irfan, M., Huang, D., Xie, J., 2017. Detection of water infiltration and deformation of unsaturated soils by elastic wave velocity. Landslides 14, 1715–1730.
Chen, Y., Irfan, M., Uchimura, T., Cheng, G., Nie, W., 2018a. Elastic wave velocity monitoring as an emerging technique for rainfall-induced landslide prediction. Landslides 15, 1155–1172.
Chen, Y., Irfan, M., Uchimura, T., Zhang, K., 2018b. Feasibility of using elastic wave velocity monitoring for early warning of rainfall-induced slope failure. Sensors 18, 997.
Chen, Y., Irfan, M., Uchimura, T., Wu, Y., Yu, F., 2019. Development of elastic wave velocity threshold for rainfall-induced landslide prediction and early warning. Landslides 16, 955–968.
Cheng, Y., Yang, J., 2005. Introduction to Environmental Geophysics. Geological Publishing House, Beijing.
Dixon, N., Spriggs, M., 2007. Quantification of slope displacement rates using acoustic emission monitoring. Can. Geotech. J. 44, 966–976.
Dixon, Neil, Meldrum, P., Smith, A., Haslam, E., Spriggs, M., Ridley, A., 2015a. Stability monitoring of a rail slope using acoustic emission. Proc. Inst. Civil Eng. Geotech. Eng. 168, 373–384.
Dixon, N., Spriggs, M.P., Smith, A., Meldrum, P., Haslam, E., 2015b. Quantification of reactivated landslide behaviour using acoustic emission monitoring. Landslides 12, 549–560.
Guo, W., Li, Y., Suo, T., 2007. A Brief Tutorial on the Fundamentals of Stress Waves. Northwestern Polytechnical University Press, Xi'an.
Guo, Z., Yin, K., Gui, L., Liu, Q., Huang, F., Wang, T., 2019. Regional rainfall warning system for landslides with creep deformation in three gorges using a statistical black box model. Sci. Rep. 9, 8962.
Han, B., Zhang, T., 2006. A study on the amplitude of elastic wave transmission in inhomogeneous media. J. Beijing Inst. Technol. (Soc. Sci. Ed.) 26, 383–387.
Huang, N.E., Shen, Z., Long, S.R., Wu, M.C., Shih, H.H., Zheng, Q., Yen, N.-C., Tung, C.C., Liu, H.H., 1998. The empirical mode decomposition and the Hilbert spectrum for nonlinear and non-stationary time series analysis. Proc. R. Soc. Lond. Ser. A: Math. Phys. Eng. Sci. 454, 903–995.
Huang, Norden E., Wu, M.-L., Qu, W., Long, S.R., Shen, S.S.P., 2003a. Applications of Hilbert-Huang transform to non-stationary financial time series analysis. Appl. Stoch. Model Bus. Ind. 19, 245–268.
Huang, Norden E., Wu, M.-L.C., Long, S.R., Shen, S.S.P., Qu, W., Gloersen, P., Fan, K.L., 2003b. A confidence limit for the empirical mode decomposition and Hilbert spectral analysis. Proc. R. Soc. Lond. Ser. A: Math. Phys. Eng. Sci. 459, 2317–2345.
Irfan, M., 2014. Elastic Wave Propagation through Unsaturated Soils Concerning Early Warning of Rain-Induced Landslides (Ph.D.). The University of Tokyo, Tokyo, Japan.
Irfan, M., Uchimura, T., 2013. Measuring shear and compression wave velocities in laboratory triaxial tests using disk shaped composite P/S piezoelectric transducer. In: IACGE 2013. Presented at the Second International Conference on Geotechnical and Earthquake Engineering. American Society of Civil Engineers, Chengdu, China, pp. 414–421.
Irfan, M., Uchimura, T., 2015. Helical filter paper technique for uniform distribution of injected moisture in unsaturated triaxial specimens. Soils Found. 55, 749–760.
Irfan, M., Uchimura, T., 2016. Modified triaxial apparatus for determination of elastic wave velocities during infiltration tests on unsaturated soils. KSCE J. Civil Eng. 20, 197–207.
Irfan, M., Uchimura, T., 2018. Development and performance evaluation of disk-type piezoelectric transducer for measurement of shear and compression wave velocities in soil. J. Earthq. Eng. 22, 147–171.
Irfan, M., Uchimura, T., Chen, Y., 2017. Effects of soil deformation and saturation on elastic wave velocities in relation to prediction of rain-induced landslides. Eng. Geol. 230, 84–94.
Li, Q., Song, D., Yuan, C., Nie, W., 2022. An image recognition method for the deformation area of open-pit rock slopes under variable rainfall. Measurement 188, 110544.
Lollino, G., Arattano, M., Cuccureddu, M., 2002. The use of the automatic inclinometric system for landslide early warning: the case of Cabella Ligure (North-Western Italy). Phys. Chem. Earth 27, 1545–1550.
Medina, V., Hurlimann, M., Guo, Z., Lloret, A., Vaunat, J., 2021. Fast physically-based model for rainfall-induced landslide susceptibility assessment at regional scale. Catena 201, 105213.
Minakov, A., Yarushina, V., 2021. Elastoplastic source model for microseismicity and acoustic emission. Geophys. J. Int. 227, 33–53.
Montoya-Domínguez, J.D., García-Aristizábal, E.F., Vega-Posada, C.A., 2016. Effect of rainfall infiltration on the hydraulic response and failure mechanisms of sandy slope models. Rev. Fac. Ing. 25, 97–109.

Notti, D., Wrzesniak, A., Dematteis, N., Lollino, P., Fazio, N.L., Zucca, F., Giordan, D., 2021. A multidisciplinary investigation of deep-seated landslide reactivation triggered by an extreme rainfall event: a case study of the Monesi di Mendatica landslide, Ligurian Alps. Landslides 18, 2341–2365.

Ochiai, H., Okada, Y., Furuya, G., Okura, Y., Matsui, T., Sammori, T., Terajima, T., Sassa, K., 2004. A fluidized landslide on a natural slope by artificial rainfall. Landslides 1, 211–219.

Uchimura, T., Towhata, I., Lan Anh, T.T., Fukuda, J., Bautista, C.J.B., Wang, L., Seko, I., Uchida, T., Matsuoka, A., Ito, Y., Onda, Y., Iwagami, S., Kim, M.-S., Sakai, N., 2010. Simple monitoring method for precaution of landslides watching tilting and water contents on slopes surface. Landslides 7, 351–357.

Uchimura, T., Towhata, I., Wang, L., Nishie, S., Yamaguchi, H., Seko, I., Qiao, J., 2015. Precaution and early warning of surface failure of slopes using tilt sensors. Soils Found. 55, 1086–1099.

Wang, J., Li, X., Hong, T., Wang, S., 2018. A semi-heterogeneous approach to combining crude oil price forecasts. Inf. Sci. 460 (461), 279–292.

Wu, L.Z., Huang, R.Q., Xu, Q., Zhang, L.M., Li, H.L., 2015. Analysis of physical testing of rainfall-induced soil slope failures. Environ. Earth Sci. 73, 8519–8531.

Wu, Y., Niu, R., Lu, Z., 2019. A fast monitor and real time early warning system for landslides in the Baige landslide damming event, Tibet, China (preprint). In: Databases, GIS, Remote Sensing, Early Warning Systems and Monitoring Technologies.

Xiao, L., Wang, J., Zhu, Y., Zhang, J., 2020. Quantitative risk analysis of a rainfall-induced complex landslide in wanzhou county, three gorges reservoir, China. Int. J. Disaster Risk Sci. 11, 347–363.

Xu, Q., Liu, H., Ran, J., Li, W., Sun, X., 2016. Field monitoring of groundwater responses to heavy rainfalls and the early warning of the Kualiangzi landslide in Sichuan Basin, southwestern China. Landslides 13, 1555–1570.

Yang, H., 2015. Empirical Mode Decomposition and its Application in Water Acoustics Signal Processing (Ph.D.). Northwestern Polytechnical University, Xi'an.

Yang, J., Wu, S., Cai, Y., 1996. Characteristics of propagation elastic waves in saturated soils. J. Vib. Eng. 9, 128–137.

Zhang, Z., 2018. Research on Elastic Wave Propagation Characteristics and Rockhurst Monitoring and Early Warning under Complex Medium Conditions (Ph.D.). China University of Mining and Technology, Beijing.

Zhang, X., Lai, K.K., Wang, S.-Y., 2008. A new approach for crude oil price analysis based on Empirical Mode Decomposition. Energy Econ. 30, 905–918.